Progress In Electromagnetics Research C, Vol. 114, 159–172, 2021

An Electrically Small Ultra-Wideband CPW-Fed Monopole Antenna

Chaluvayalil Vinisha, Sruthi Dinesh, Rajan Vivek, Karavilavadakkethil C. Prakash, Chandroth Aanandan, Kesavath Vasudevan, and Pezholil Mohanan*

Abstract—An electrically small ultra-wideband (UWB) antenna to cater to the need for UWB communication suitable for today's small gadgets is presented. The antenna is realized on a substrate of relative dielectric permittivity 4.4, loss tangent 0.02, and height 1.6 mm. The overall dimension of the antenna is 21 mm × 16 mm × 1.6 mm ($0.217\lambda_{\min} \times 0.165\lambda_{\min} \times 0.0165\lambda_{\min}$), where $\lambda_{\min}$ is the wavelength corresponding to the antenna's lowest operating frequency in free-space 3.1 GHz. The small '$k_{\min}a$' value of 0.856 of the antenna, where $k_{\min}$ is the wavenumber corresponding to $\lambda_{\min}$, and 'a' is the radius of the sphere that can fully enclose the antenna, is electrically small. The antenna operates at the FCC recommended UWB frequency range from 3.1 GHz to 10.6 GHz with a reasonably good 2 : 1 voltage standing wave ratio (VSWR) impedance bandwidth. A prototype of the proposed antenna is fabricated, and different radiation characteristics of the antenna in the frequency and time domain are measured and validated by simulation. The high pulse fidelity for different antenna orientations and very small group delay in the operating frequency band exhibit insignificant pulse distortion. The equivalent isotropically radiated power (EIRP) of the antenna satisfies the FCC mask in the entire UWB. The maximum gain and efficiency achieved within the UWB are 3.95 dBi and 93%, respectively. Radiation characteristics of the antenna in the UWB are studied in an anechoic chamber using Agilent PNA E 8362B.

1. INTRODUCTION

Ultra-wideband (UWB) finds wide applications in communication due to the requirement of high data rate, low power consumption, and low multipath interferences. The recommendation of unlicensed-UWB by Federal Communications Commission (FCC) from 3.1 GHz to 10.6 GHz [1] for communication has triggered antenna engineers to develop compact and efficient antennas in this band. A UWB antenna used for this type of communication has to fulfil different stringent electromagnetic criteria like large impedance bandwidth, high fidelity, good efficiency, moderate gain, omnidirectional radiation pattern along with equivalent isotropically radiated power (EIRP) limitations of preserving the shapes of transmitted and received pulses in time and frequency domains.

Several types of monopole patch antennas are available [2–4] satisfying UWB responses. Tapering, defecting, and etching out a U slit in the microstrip feed of the partial ground plane of the antenna are considered [2] to improve the bandwidth. In [3], a UWB is achieved by connecting the feeding network of the hybrid slot — where the slot is made up of an open-ended rectangle and a closed-ended circle — to an inverted L-shape with circular corner. A ring-shaped structure with an additional slot and upper cutting edge is used to achieve the UWB [5]. However, these antennas are relatively high in profile and not suitable for the present compact slim UWB gadgets. This study aims to develop an electrically small UWB antenna satisfying all the radiation characteristics without using any lumped elements for matching.

Received 18 April 2021, Accepted 22 July 2021, Scheduled 9 August 2021

* Corresponding author: Pezholil Mohanan (drmohan@gmail.com).
The authors are with the Centre for Research in Electromagnetics and Antennas, Department of Electronics, Cochin University of Science and Technology, Cochin, Kerala 682022, India.

In this paper, a novel co-planar waveguide (CPW) fed monopole antenna with an omnidirectional radiation pattern is proposed. The antenna is simple, electrically small and provides all the radiation characteristics as envisaged by FCC for UWB communication. The antenna is made up of a vertically striped annular ring-shaped monopole with CPW feed. The structure is very small in size, $21\,\text{mm} \times 16\,\text{mm} \times 1.6\,\text{mm}$ with an electrical dimension of $0.217\lambda_{\min} \times 0.165\lambda_{\min} \times 0.0165\lambda_{\min}$, where $\lambda_{\min}$ is the wavelength at the lowest frequency of operation in free-space. The dimensions of the antenna elucidates that the antenna is electrically small and can be mounted on a finite space with the lowest $k_{\min}a = 0.856$ (where a is the Chu sphere radius that can circumscribe the antenna [6]). The antenna exhibits a UWB frequency response ranging from 3.1 GHz to 10.6 GHz for a 2 : 1 VSWR impedance bandwidth. Also, the antenna exhibits excellent radiation performance in the time and frequency domains as illustrated in this paper. The performance of the proposed antenna is also compared with the existing similar antennas in the literature. From the simulation and experimental studies, the proposed antenna can be an ideal choice for applications that require electrically small antennas for UWB.

2. ANTENNA DESIGN

The schematic layout and geometry of the proposed antenna are as shown in Fig. 1. The patch and CPW transmission line are etched on the same plane of a substrate with permittivity, $\varepsilon_r = 4.4$, loss tangent $\tan\delta = 0.02$, and thickness $h = 1.6\,\text{mm}$. Schematic top view and side view of the proposed antenna are presented in Fig. 1(a) and Fig. 1(b). The structure of the proposed antenna has evolved from the basic CPW-fed disc monopole antennas [7, 8] and is depicted in Fig. 2.

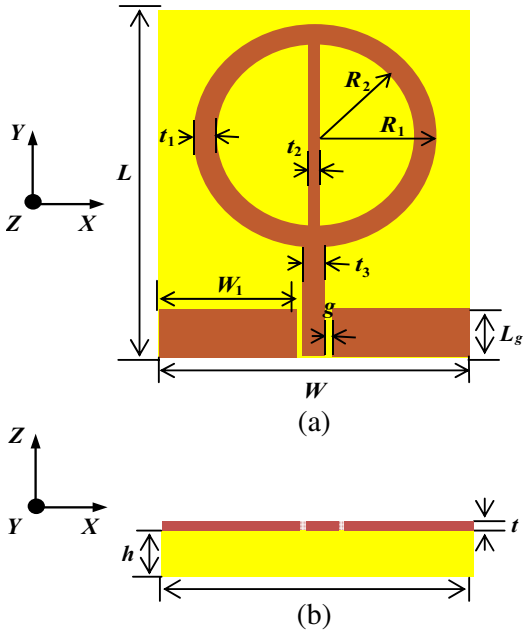

Figure 1. Schematic view of the proposed antenna. (a) Top-view. (b) Side-view.

In the proposed design, a vertically striped annular ring structure is fed by the CPW transmission line. The width of the annular ring, $R_1 - R_2 = t_1$, is also kept the same as that of the central line CPW transmission line, t_3. The gap between the transmission line and the ground plane, 'g', is kept 0.6 mm after optimisation. W_1 and L_g are the lengths of the ground plane in X and Y directions.

The outer ring radius $R_1 = 0.1 \times \lambda_{g\,\min}$ where $\lambda_{g\,\min}$ is the guided wavelength of the proposed

antenna at the lowest frequency of operation and calculated using the following equations [9],

$$\lambda_g = \frac{\lambda_{\min}}{\sqrt{\varepsilon_{eff}}} \tag{1}$$

$$\varepsilon_{eff} \simeq \frac{\varepsilon_r + 1}{2}, \tag{2}$$

where $\lambda_{\min}$ is the free-space wavelength at the lowest frequency of operation, and ε_{eff} is the effective dielectric permittivity of the medium.

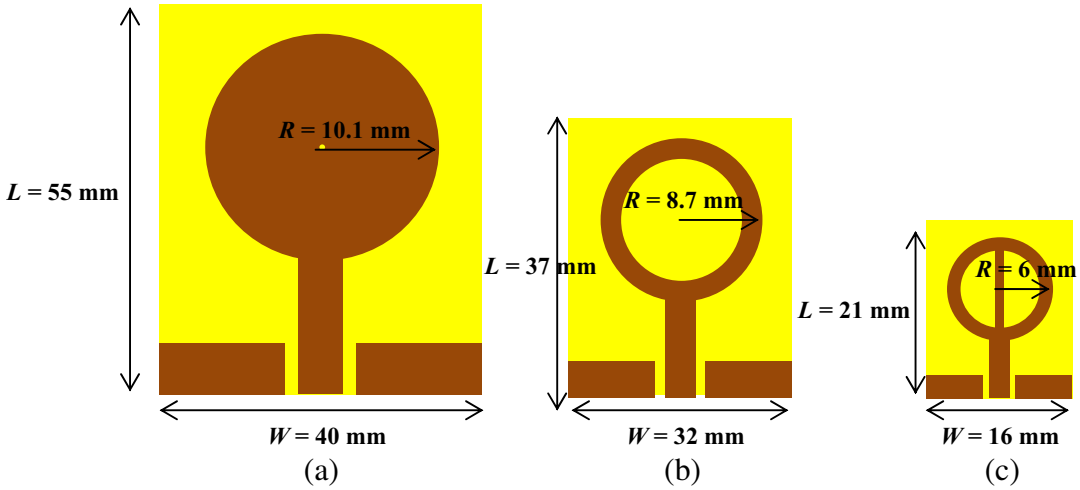

Figure 2. Evolution steps of the proposed antenna.

Ansys High-Frequency Structure Simulator (HFSS) has been used for simulation studies. All parameters are optimised for the antenna to radiate in the FCC recommended UWB bandwidth. The overall dimension of the proposed antenna is 21 mm × 16 mm × 1.6 mm. Optimised antenna parameters for the proposed antenna are given in Table 1.

Table 1. Optimised parameters for the proposed antenna.

Optimised Parameter	Value (in mm)
L	21
W	16
R_1	6
T_1	2
T_2	1
T_3	2
W_1	6.4
L_g	4.1
G	0.6

For the proposed antenna, the ka value is found to be 0.86, which is less than one, thus can be considered as an electrically small antenna (ESA), where k is the wave number (rad/m), $2\pi/\lambda$, and 'a' is the radius of the smallest sphere that can enclose the maximum dimension of the proposed antenna according to Chu [6]. According to [10], the UWB antenna can be considered as an ESA if it satisfies

the condition $a_1 < \lambda_0/5$, where a_1 is the size of the radiating element, which is 12 mm. Thus, the proposed antenna has $a_1 = 12$ mm, which is again less than $\lambda_0/5$ hence can be treated as an electrically small UWB antenna.

The evolution of the proposed antenna is shown in Fig. 2. The basic structure is the CPW-fed circularly shaped monopole patch antenna, shown in Fig. 2(a). This antenna radiates from 2.2 GHz to 10.6 GHz [4] with an overall dimension of 55 mm × 40 mm. Even though the antenna works in the UWB, the antenna is not compact. Next in the evolution, annular ring antenna is considered by eliminating the central part of the circular patch antenna as shown in Fig. 2(b) [7]. This antenna radiates from 2.38 GHz to 3.36 GHz with an overall dimension of 37 mm × 32 mm [7]. A vertical strip at the central line of the annular ring is introduced in the proposed antenna for further miniaturisation of the antenna by allowing the current to split and combine within the region, thus improving the electrical dimensions, hence results improved bandwidth for that particular physical size of the antenna compared to conventional designs. The new band is from 3.1 GHz to 10.6 GHz with an overall dimension of 21 mm × 16 mm.

For the study, three antennas in the evolution having the same outer dimensions are considered. As shown in the return loss plot, there is an improvement in the bandwidth for the proposed antenna with the same dimensions in the evolution. The return losses of the three types of antennas are compared in Fig. 3. It can be observed from the figure that, by introducing the vertical strip, there is a remarkable improvement in the bandwidth of the proposed antenna without changing the dimension.

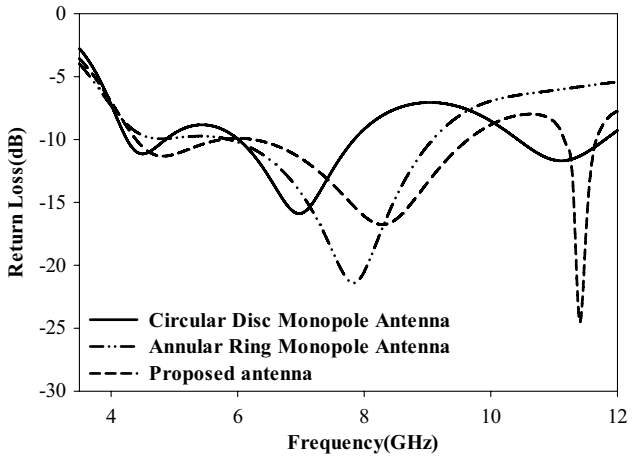

Figure 3. Return loss comparison plot for antennas having same outer dimensions.

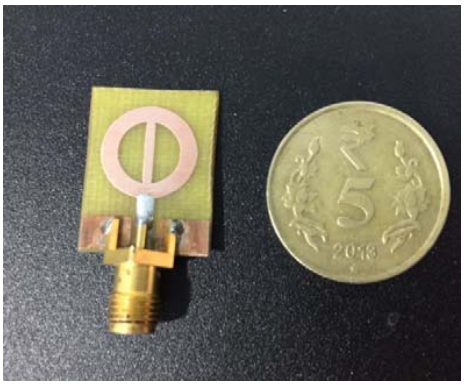

Figure 4. Photograph of the fabricated antenna.

Table 2. Substrate properties along with the calculated dimensions of the antenna.

	Antenna I	**Antenna II**	**Antenna III**	**Antenna IV**
ε_r	2.2	4.4	6.15	10.2
h (mm)	1.6	1.6	1.6	1.6
R (mm)	7.8	6	5.3	4.5
G (mm)	0.17	0.6	0.45	0.5
T_3 (mm)	4	2	2.58	2.05

Table 2 shows the substrate properties along with the calculated antenna dimensions for various substrates. R, G, and t_3 are computed as per the design equations. Using Ansoft HFSS, all other parameters are optimised for these antennas and tabulated in Table 3. This validates the design equations for the antenna on different substrates.

Table 3. Substrate properties along with the optimised dimensions of the antenna.

	Antenna I	**Antenna II**	**Antenna III**	**Antenna IV**
ε_r	2.2	4.4	6.15	10.2
h (mm)	1.6	1.6	1.6	1.6
W (mm)	18.2	16	11.6	15
L (mm)	22.7	21	18.3	17
R (mm)	7.8	6	5.3	4.5
G (mm)	0.17	0.6	0.45	0.5
T_1 (mm)	4	2	2.58	2.05
T_2 (mm)	1	1	1	1
T_3 (mm)	4	2	2.58	2.05

A photograph of the fabricated antenna is shown in Fig. 4. The measured and simulated return losses of the antenna are shown in Fig. 5. Measurement of the antenna return loss is performed using PNAE-8362B vector network analyser. It can be observed that the antenna provides a good 2 : 1 VSWR return loss in the FCC recommended bandwidth, 3.1 GHz to 10.6 GHz. The measured and simulated return losses are in close agreement.

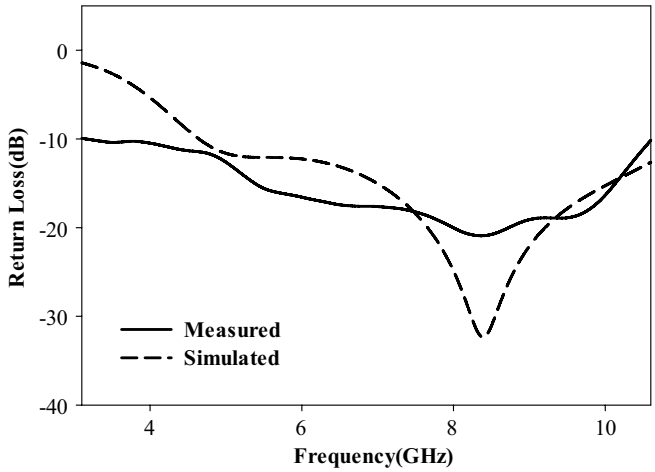

Figure 5. Simulated and measured return losses of the proposed antenna.

As seen from Fig. 3, there are three resonances for this antenna. Eventually, these three resonances merge to form a UWB.

The current distributions at 4 GHz, 6 GHz, 8 GHz are as shown in Figs. 6(a)–(d), respectively. It can be observed from the current distribution that by introducing a vertical strip to the annular ring, the current gets divided equally into the two strips at the junction and then combines at the other end and passes through the vertical strip downwards. So, the electrical length will increase, and the antenna will be able to accommodate larger wavelengths than before. The ring structure contributes to the radiation throughout the bandwidth range, whereas at higher frequencies, the center strip shows the highest current, which implies that the center-strip contributes mainly towards the higher resonances.

The antenna parameters for various substrates are computed in order to substantiate the design equations. Simulated antenna return losses on various substrates are illustrated in Fig. 7. Other antenna parameters are also studied for the proposed antenna.

The outer radius of the annular ring plays a vital role in the overall resonant frequencies of the antenna. The dimension of the outer radius of the ring is inversely proportional to the lowest

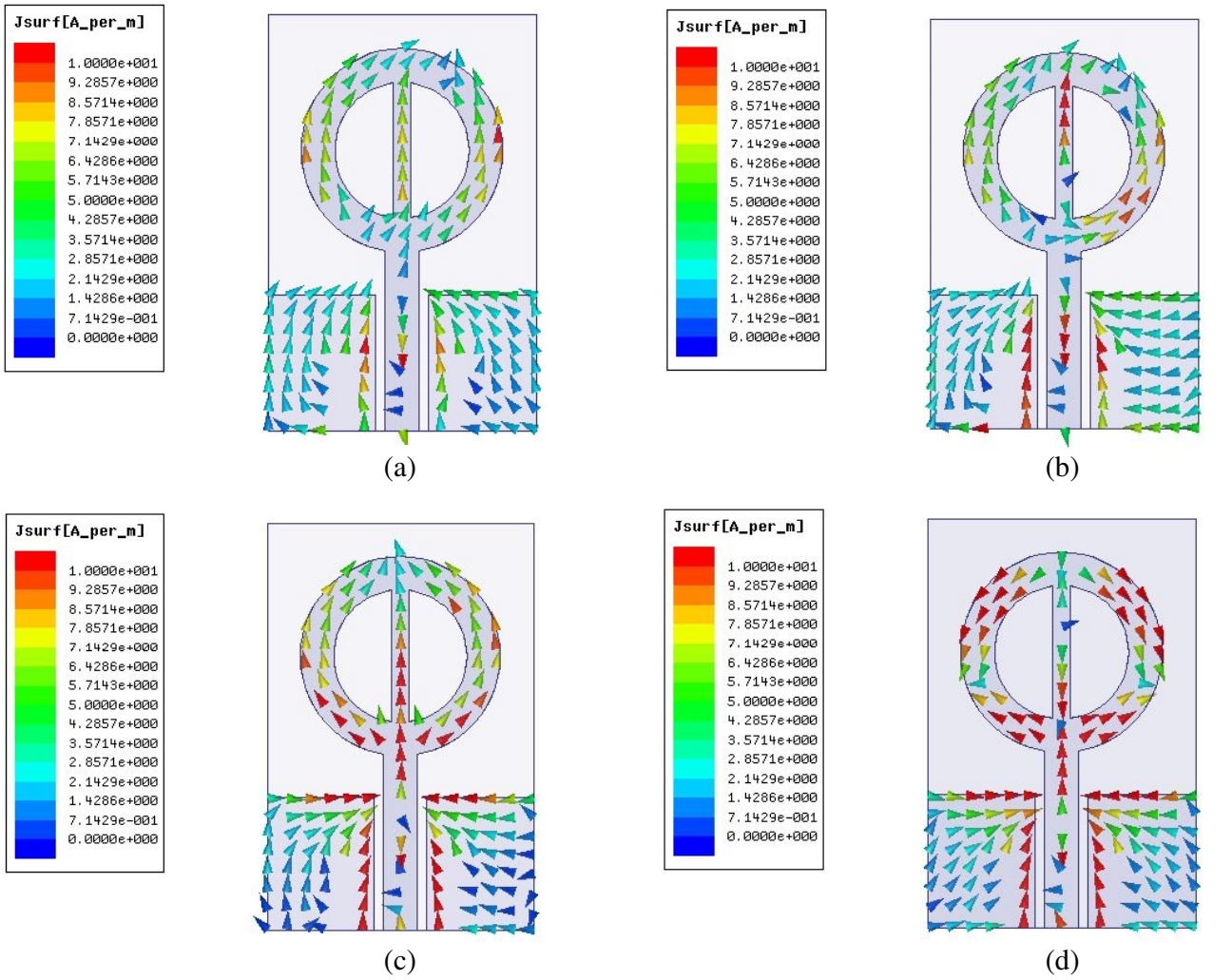

Figure 6. Current distribution of the proposed antenna at (a) 4 GHz, (b) 6 GHz, (c) 8 GHz and (d) 10 GHz respectively.

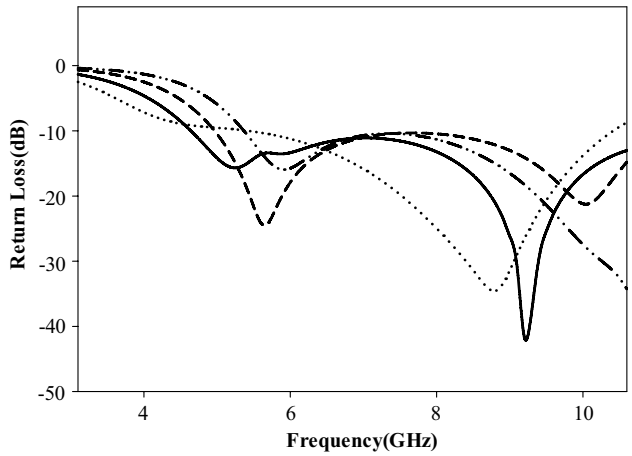

Figure 7. Return loss of the antenna with different substrate parameters.

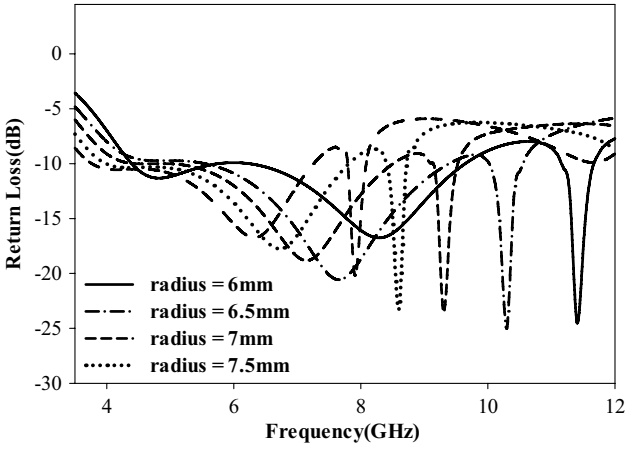

Figure 8. Impedance bandwidth variation w.r.t outer radius of the annular ring.

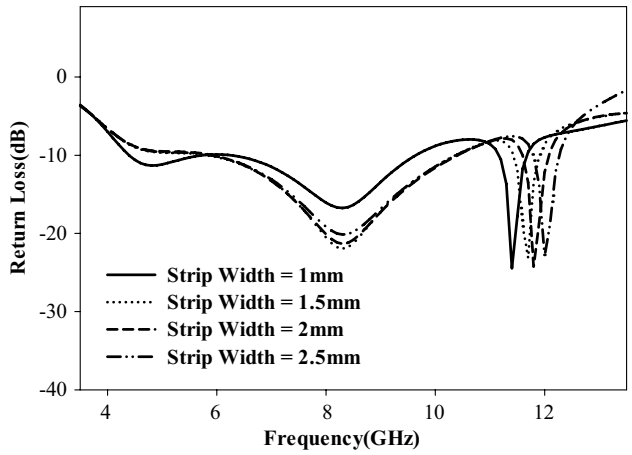

Figure 9. Impedance bandwidth variation w.r.t width of vertical strip.

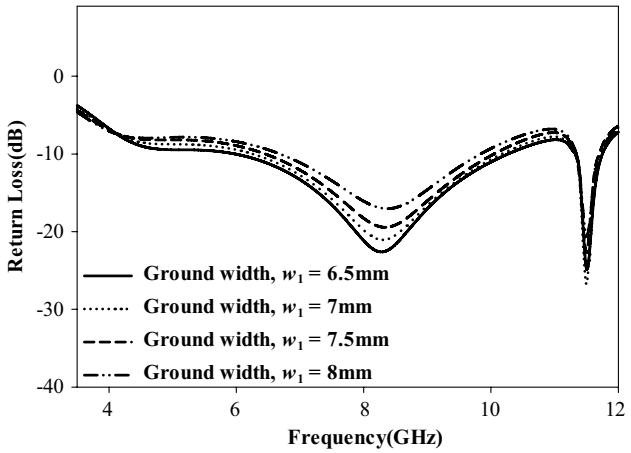

Figure 10. Impedance bandwidth variation w.r.t ground width, W_1.

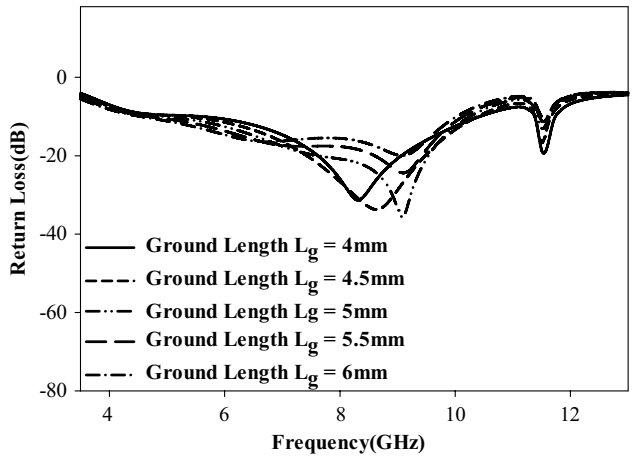

Figure 11. Impedance bandwidth variation w.r.t ground length, L_g.

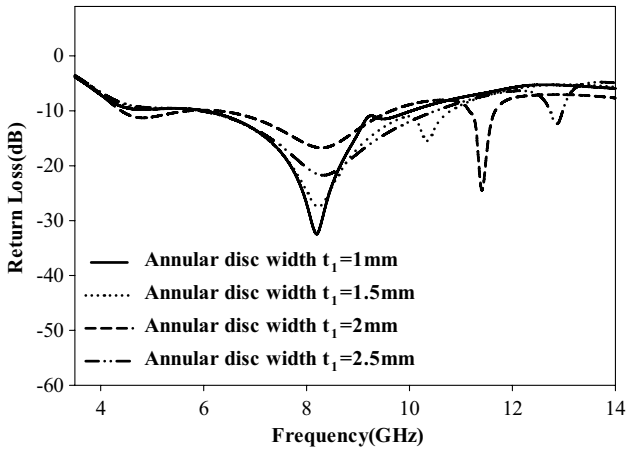

Figure 12. Impedance bandwidth variation w.r.t annular disc width, t_1.

operating frequency of the antenna. So, when the outer radius of the ring is increased, the structure can accommodate much larger wavelengths without distortion, i.e., the guided wavelength, and thus the resonance frequency gets shifted towards the lower band. The variation in the resonant frequencies with respect to the outer radius is illustrated in Fig. 8.

The performance of the antenna with width of the vertical strip (t_2 is varied from 1 mm to 2.5 mm by 0.5 mm, while all other parameters, $R_1 = 6$ mm, $t_1 = t_3 = 2$ mm, $L = 21$ mm, $W = 16$ mm, are kept constant) is illustrated in Fig. 9. When the width of the transmission line is increased, the inductance value of the transmission line is increased, the capacitance value within the two gaps inside the ring also varied, and thus there is a slight variation in the antenna resonant frequency. It is found that, as the strip width is increased, the return loss for the second harmonic gets improved, and the third harmonic gets shifted towards a higher frequency. An optimal value of 1 mm strip width is selected for the fabrication. However, at the same time, an improved fundamental resonance is observed for a vertical strip-width of 1 mm.

The changes in antenna return loss with the length of the ground plane along the X direction are illustrated in Fig. 10. It is noticed that the bandwidth of the antenna is virtually independent of the length of the ground plane.

The effect of the width of the ground plane in the Y direction, L_g, on the resonant frequencies is also studied. When width is increased, the transmission line length also gets increased, and the inductance and capacitance values between the signal and the ground also get changed, and thus the resonant frequencies in the second harmonic undergo notable variations. A new resonance is visible in the operating band, which indicates that two resonances get merged to result in a much larger second harmonic. This is illustrated in Fig. 11.

In the parametric study, the width of the annular disc, t_1, is included. t_1 is varied from 1 mm to 2.5 mm by 0.5 mm in the study. As illustrated in Fig. 12, it can be inferred that the third resonance gets more influenced by this width. The fundamental harmonic return loss level gets better when t_1 is increased, and the overall bandwidth gets improved. Even though the second harmonic return loss is reduced, it is in the permissible range.

Radiation patterns of the proposed antenna at regular intervals are studied, and measurements

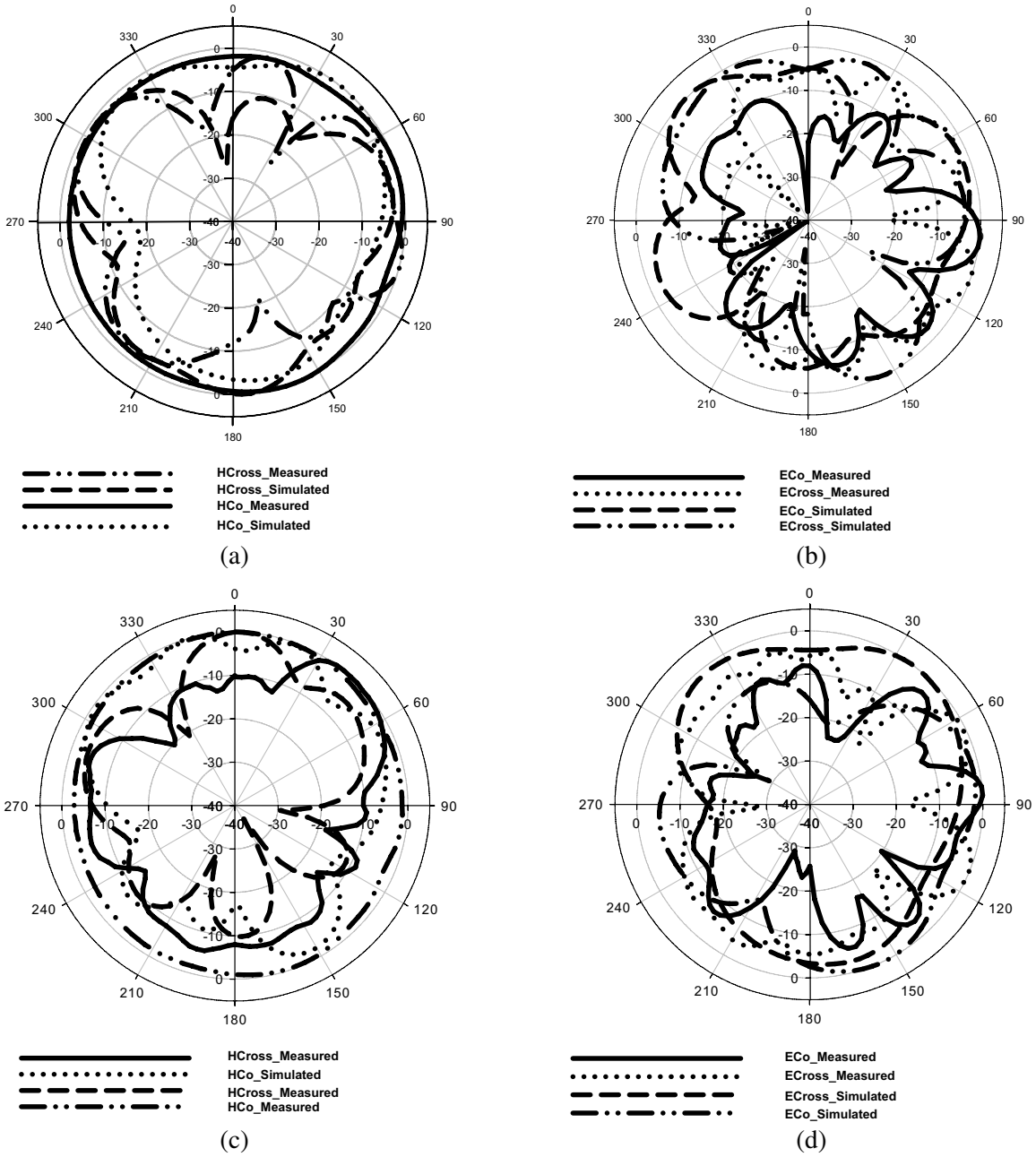

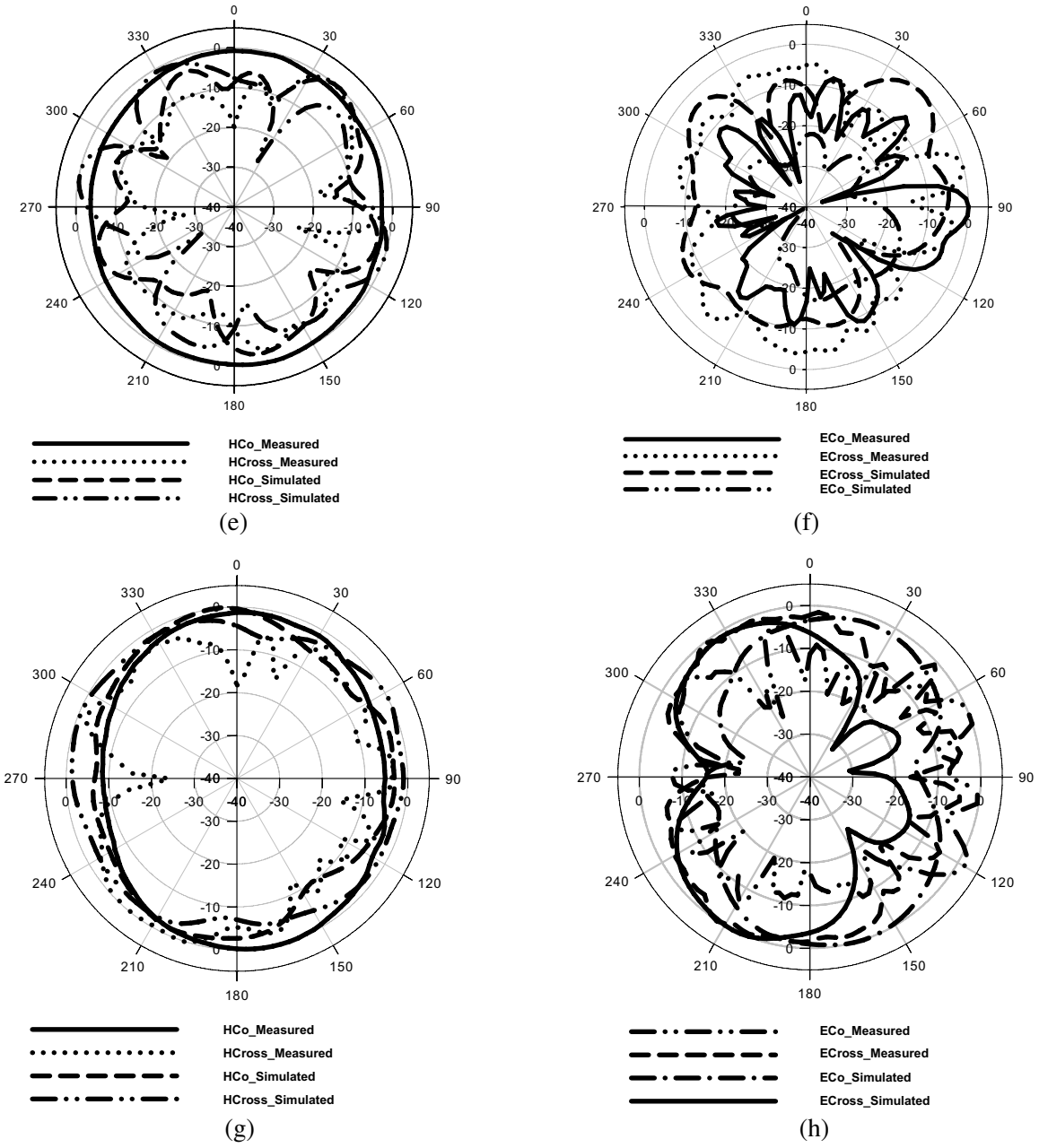

Figure 13. Co-polarised and cross-polarised radiation patterns of the proposed antenna at (a)&(b), 4 GHz, (c)&(d), 6 GHz, (e)&(f), 8 GHz, (g)&(h), 10 GHz respectively.

are performed in an indoor anechoic chamber. Fig. 13 illustrates the measured and simulated co- and cross-polarised radiation patterns in the H-plane and E-plane of the antenna at 4 GHz, 6 GHz, 8 GHz, and 10 GHz, respectively. The antenna is polarised in the Y direction with nearly an omnidirectional pattern. As the frequency gets increased, the E-plane as well as H-plane patterns start deteriorating. The antenna ensures better cross polarisation in the entire frequency band. The measured patterns are in good agreement with the simulated radiation patterns.

The gain-comparison method is used to measure the gain of the proposed antenna. The proposed antenna offers a better gain in the operating band which is illustrated in Fig. 14 and shows a peak gain of 3.95 dB at 10.5 GHz.

Wheeler cap method [11–14] is used to measure the efficiency of the proposed antenna. The

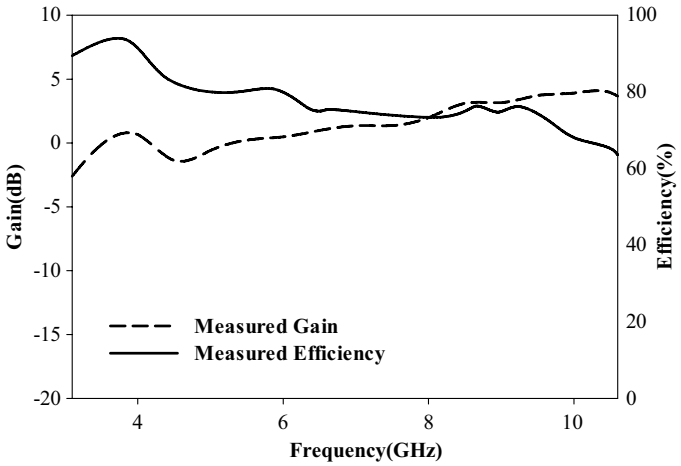

Figure 14. Gain and efficiency of the proposed antenna.

efficiency of the proposed antenna over the band is also shown in Fig. 14. The average efficiency over the UWB is found to be 74.52% whereas the maximum efficiency of 93.82% is obtained at 3.5 GHz.

3. TIME DOMAIN ANALYSIS

In the case of UWB antennas, time domain analysis is important since the antenna radiates over a very wide band, and frequency domain analysis alone is not sufficient to substantiate the performance of the antenna over the entire bandwidth. It is vital to do the transient analysis such as group delay, likenesses of the input and received waveform shapes, fidelity factor, and EIRP (Equivalent Isotropically Radiated Power) of the antenna.

For this study, two identical antennas are fabricated, and the transfer characteristics of the antenna in free space are studied to investigate the pulse handling capabilities of the proposed antenna [15]. Two antennas are placed apart at a distance (R) of 100 mm which satisfies the far-field criteria for the antennas, and the scattering parameters are measured for the face-to-face and side-by-side orientations of the antennas. It is demonstrated in Fig. 15. The antenna is modelled by its transfer function, and the transfer function of the antenna at any angular frequency, ω, is evaluated from the following expression from the measured $S_{21}(\omega)$,

$$H(\omega) = \sqrt{\frac{2\pi RcS_{21}(\omega)e^{j\omega R/C}}{j\omega}} \tag{3}$$

A fourth-order derivative of the Rayleigh function is considered to arrive at the prototype receiving

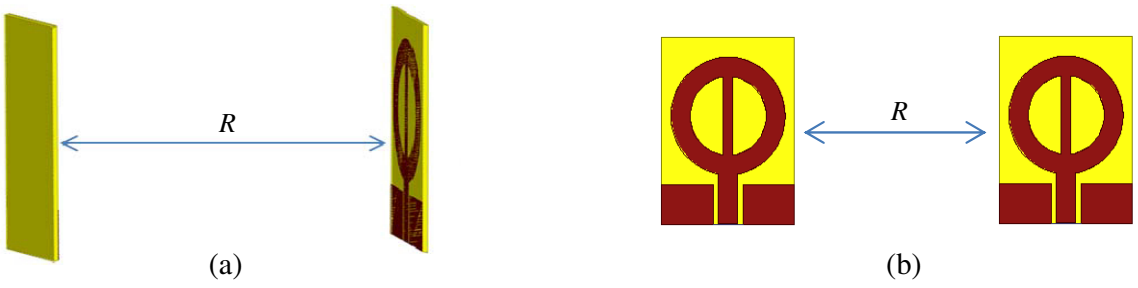

Figure 15. Demonstration of (a) face-to-face and (b) side-by-side method for the group delay measurement.

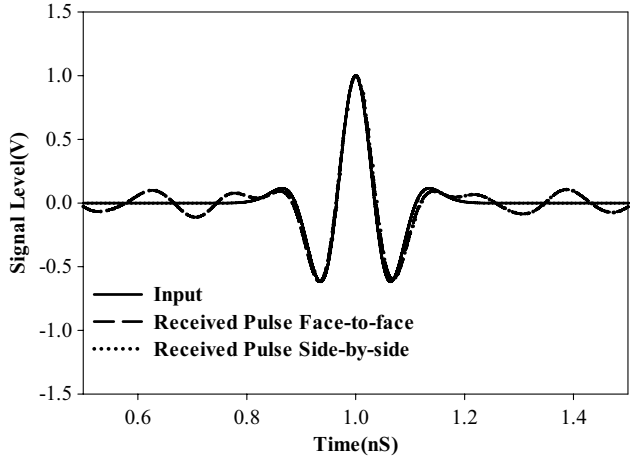

Figure 16. Input and received pulse of the proposed antenna.

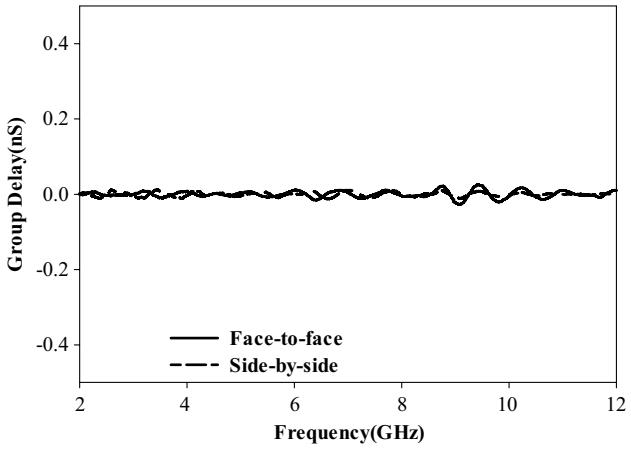

Figure 17. Group delay of the proposed antenna for face-to-face and side-by-side orientations.

antenna, and the transmitted fourth order time domain Rayleigh pulse is expressed as,

$$S_t(t) = \frac{16x^4 - 48x^2 + 120}{\sqrt{2\pi}} \text{ V/m} \tag{4}$$

By taking the linear convolution sum of the transmitted signal, $S_t(t)$, and the time-domain transfer function of the antenna, $|H_t(t)|$, the output waveform from the receiving prototype antenna terminal is expressed as,

$$S_r(t) = S_t(t) \otimes H(t) \text{ V/m} \tag{5}$$

The likenesses in the shapes of the input waveform and the received waveform for the face-to-face and side-by-side antenna orientations are illustrated in Fig. 16, and it is evident that the received waveforms preserve the shape of the input Rayleigh waveform. It is observed that the ringing effect is negligible for the two orientations, and these two waveforms follow the same shape.

Group delay measurements for the UWB antennas are vital in establishing the non-distorted characteristic of the structure. An invariant group delay indicates that the antenna is non-resonant in nature, and thus the antenna radiates [10].

Two identical-prototype antennas are used for the measurement of the group delay, and group delay is measured for face to face and side by side orientations. The measured group delay is depicted in Fig. 17. It is observed that the group delay variations are less than 2 nS and are almost linear in the entire UWB frequency range which indicates the non-resonant characteristic of the proposed antenna [10].

Another significant parameter to be studied while the transient analysis is performed is the fidelity factor, which evaluates the correlation of the shapes between the transmitted and received waveforms irrespective of their magnitude and time delay [16].

Fidelity factor can be computed from the normalized transmitted and received signals, and the fidelity factor is expressed as [16],

$$F = \max_{\tau} \int_{-\infty}^{\infty} \hat{S}_t(t)\hat{S}_r(t+\tau)dt \tag{6}$$

where,

$$\hat{S}_r(t) = \frac{S_r(t)}{\left[\int_{-\infty}^{\infty} |S_t(t)|^2\right]^{1/2}} \tag{7}$$

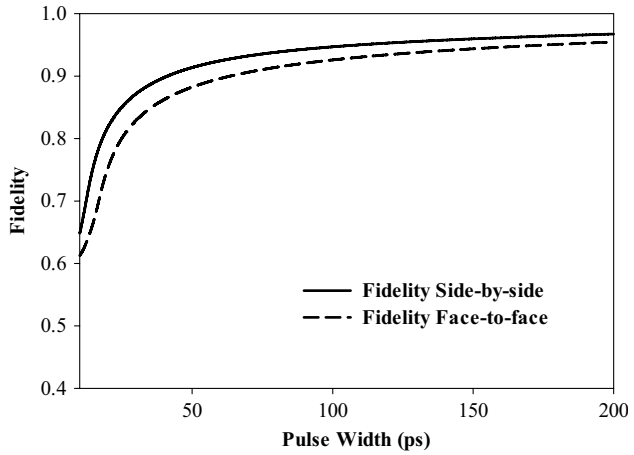

Figure 18. Fidelity factor of the proposed antenna.

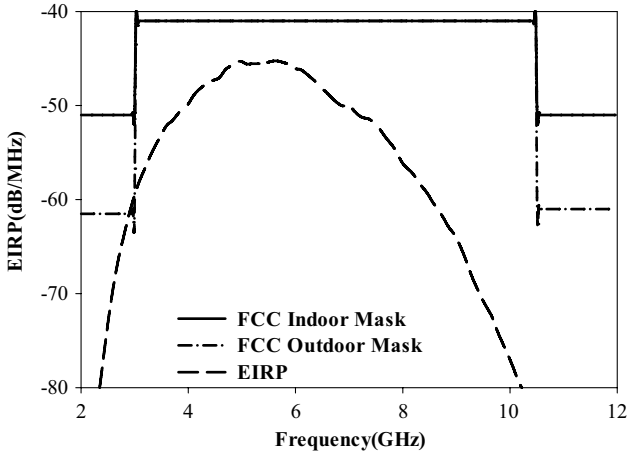

Figure 19. EIRP of the proposed antenna.

$$\hat{S}_t(t) = \frac{S_t(t)}{\left[\int_{-\infty}^{\infty} |S_r(t)|^2\right]^{1/2}} \tag{8}$$

The fidelity factor varies from 0 to 1. The fidelity factor close to one indicates better signal handling capability of the proposed antenna and negligible dispersion of the transmitted signal. The measured fidelity factor of the antenna for face-to-face antenna orientation is 0.890, and that of side-by-side antenna orientation is 0.912. The fidelity factor close to one indicates better signal handling capability of the proposed antenna and negligible dispersion of the transmitted signal. Less than 0.5 fidelity factors indicate less resemblance to the received signal from that of the transmitted pulse. The fidelity factor of the proposed antenna is as illustrated in Fig. 18.

The next parameter to be evaluated is the EIRP (Equivalent Isotropically Radiated Power) of the proposed antenna. FCC recommended that spectral masks are used to investigate whether the antenna satisfies the stringent requirements of FCC in the interested frequency band. EIRP is defined as the amount of power that would have to be emitted by anisotropic antenna in-order to produce the peak

Table 4. Comparison table of proposed antenna and previous works.

Reference	Dimensions (λ_{min}) (mm)	VSWR	Operation Bandwidth (GHz)	Fractional Bandwidth (BW/fc)	$k_{min}a$	Peak Gain (dBi)
[3]	$21 \times 26 \times 0.8$	2	3.03–11	113.6137	1.06	-
[20]	$25 \times 20 \times 1.6$	2	2.86–16.17	139.8844	0.958	5.27
[4]	$43 \times 34 \times 1.6$	2	2.2–10.6	131.2500	1.26	3
[2]	$32 \times 32 \times 1.6$	2	2.9–15	135.1955	1.37	4.85
[21]	$22 \times 19 \times 1.6$	2	4.5–20	126.5306	1.37	6.3
[5]	$35 \times 24 \times 1.6$	2	3.088–2.497	120.7443	1.37	6.8
[22]	$19.2 \times 28.8 \times 1.6$	2	3.4–14	121.8391	1.23	6
[23]	$30 \times 27 \times 1.6$	2	2.7–12	126.53	1.14	5
[24]	$17.7 \times 26 \times 1.6$	2	3.1–10.6	109.49	1.02	3.2
Proposed antenna	$\mathbf{21 \times 16 \times 1.6}$	**2**	**3.1–10.6**	**109.4891**	**0.856**	**3.95**

power density of the device under test. EIRP is meant to restrict the radiation power from wireless devices, and it is expressed as EIRP $= G_T(f) \times P_T(f)$ where $G_T(f)$ is the peak gain of the transmitting antenna, and $P_T(f)$ is the transmitter power density [17–19]. EIRP of the antenna is calculated using,

$$\text{EIRP} = P_T(f) \times \sqrt{H(\omega)} \times [4\pi Rf/c] \tag{9}$$

The excitation signal used for the measurement is a fourth order Rayleigh pulse with a pulse width factor, 50 ps. The results are shown in Fig. 19. From the results, it is observed that the proposed antenna satisfies the FCC mask limitations for the entire band of performance.

Features of the proposed UWB ESA antenna have been compared with the previous works published in various journals. For this, dimensions of the antenna, VSWR, operation bandwidth of the antenna, fractional bandwidth, $k_{\min}a$, and the peak gain of the antennas are considered. It is formulated in Table 4. The proposed antenna covers the FCC recommended bandwidth, and it satisfies all other criteria put forward by FCC. Compared to the other antennas in Table 4, the proposed antenna is very compact in size and comes under the Chu limit. The antenna has an intermediate gain and bandwidth as compared to other antennas listed in Table 4.

4. CONCLUSION

In this paper, an electrically small UWB antenna for wireless communication is presented. The performance of the proposed antenna is compared with existing miniature UWB antennas. Indoor antenna measurements are performed, and time and frequency domain analyses of the proposed antenna are presented. The antenna satisfies all the FCC recommended radiation characteristics. In the time domain analysis, better fidelity factors for side-by-side orientation and face-to-face orientations are observed. The received pulse of the antenna preserves the shape as that of the transmitted pulse, ensuring the EIRP limitations recommended by FCC. Thus, the proposed electrically small-ultra wideband antenna is considered to be suitable for aerodynamic application where light weight is a major criterion.

REFERENCES

1. Siwiak, K. and D. McKeown, *Ultra-wideband Radio Technology*, Wiley, 2004.
2. Mohandoss, S., R. R. Thipparaju, B. N. Balarami Reddy, S. K. Palaniswamy, and P. Marudappa, "Fractal based ultra-wideband antenna development for wireless personal area communication applications," *AEU — Int. J. Electron. Commun.*, Vol. 93, 95–102, Sep. 2018.
3. Zong, W.-H., et al., "A compact slot antenna for UWB applications," *2016 IEEE MTT-S International Wireless Symposium (IWS)*, 1–4, 2016.
4. Abdelraheem, A. M. and M. A. Abdalla, "Compact curved half circular disc-monopole UWB antenna," *Int. J. Microw. Wirel. Technol.*, Vol. 8, No. 2, 283–290, Mar. 2016.
5. Hossain, M. J., M. R. I. Faruque, and M. T. Islam, "Design of a patch antenna for ultra wide band applications," *Microw. Opt. Technol. Lett.*, Vol. 58, No. 9, 2152–2156, Sep. 2016.
6. Chu, L. J., "Physical limitations of omni-directional antennas," *J. Appl. Phys.*, Vol. 19, No. 12, 1163–1175, Dec. 1948.
7. Oraizi, H. and B. Rezaei, "Improvement of antenna radiation efficiency by the suppression of surface waves," *J. Electromagn. Anal. Appl.*, Vol. 3, No. 3, 79–83, 2011.
8. Allen, B., M. Dohler, E. E. Okon, W. Q. Malik, A. K. Brown, and D. J. Edwards, *Ultra-wideband*, John Wiley & Sons, Ltd, Chichester, UK, 2006.
9. Balanis, C. A., *Antenna Theory: Analysis and Design*, 4th Edition, Wiley, 1997.
10. Wiesbeck, W., G. Adamiuk, and C. Sturm, "Basic properties and design principles of UWB antennas," *Proc. IEEE*, Vol. 97, No. 2, 372–385, Feb. 2009.
11. Kulkarni, J. and C.-Y.-D. Sim, "Wideband CPW-fed oval-shaped monopole antenna for Wi-Fi5 and Wi-Fi6 applications," *Progress In Electromagnetics Research C*, Vol. 107, 173–182, 2021.

12. Kulkarni, J., N. Kulkarni, and A. Desai, "Development of 'H-Shaped' monopole antenna for IEEE 802.11a and HIPERLAN2 applications in the laptop computer," *Int. J. RF Microw. Comput. Eng.*, Vol. 30, No. 7, Jul. 2020.
13. Kulkarni, J. and C. Sim, "Multiband, miniaturized, maze shaped antenna with an air-gap for wireless applications," *Int. J. RF Microw. Comput. Eng.*, Vol. 31, No. 1, Jan. 2021.
14. Wheeler, H., "The radiansphere around a small antenna," *Proc. IRE*, Vol. 47, No. 8, 1325–1331, Aug. 1959.
15. Duroc, Y., A. Ghiotto, T. P. Vuong, and S. Tedjini, "UWB antennas: Systems with transfer function and impulse response," *IEEE Trans. Antennas Propag.*, Vol. 55, No. 5, 1449–1451, May 2007.
16. Quintero, G., J.-F. Zurcher, and A. K. Skrivervik, "System fidelity factor: A new method for comparing UWB antennas," *IEEE Trans. Antennas Propag.*, Vol. 59, No. 7, 2502–2512, Jul. 2011.
17. Oh, S.-S. and Y.-H. Lee, "An EIRP measurement method for base-station antennas using field strengths measured along a single straight line," *Int. J. Antennas Propag.*, Vol. 2013, 1–6, 2013.
18. Pozar, D. M., *Microwave Engineering*, 4th Edition, Wiley, 2011.
19. Mirshafiei, M., M. Abtahi, S. LaRochelle, and L. A. Rusch, "Wideband antenna EIRP measurements for various UWB waveforms," *2008 IEEE International Conference on Ultra-Wideband*, 125–128, 2008.
20. Tiwari, R. N., P. Singh, and B. K. Kanaujia, "Small-size Scarecrow-shaped CPW and microstrip-line-fed UWB antennas," *J. Comput. Electron.*, Vol. 17, No. 3, 1047–1055, Sep. 2018.
21. Touhami, N. A., Y. Yahyaoui, A. Zakriti, K. Bargach, M. Boussouis, M. Lamsalli, and A. Tribak, "A compact CPW-fed planar pentagon antenna for UWB applications," *Progress In Electromagnetics Research C*, Vol. 46, 153–161, 2014.
22. Chattoraj, N., "Design and development of a small compact ultra wideband antenna," *IOP Conf. Ser. Mater. Sci. Eng.*, Vol. 44, 012003, Apr. 2013.
23. Jacob, S., V. A. Shameena, S. Mridula, C. K. Anandan, K. Vasudevan, and P. Mohanan, "Planar UWB antenna with modified slotted ground plane," *Int. J. RF Microw. Comput. Eng.*, Vol. 22, No. 5, 594–602, Sep. 2012.
24. Shameena, V. A., M. Manoj, M. Remsha, C. V. Vinisha, and P. Mohanan, "CPW fed ultra wideband strip antenna," *2019 URSI Asia-Pacific Radio Science Conference (AP-RASC)*, 1–4, 2019.